Parity nonconservation in polarized-neutron transmission through ^{139}La

V. W. Yuan,[1] C. D. Bowman,[1] J. D. Bowman,[1] J. E. Bush,[2] P. P. J. Delheij,[3] C. M. Frankle,[2] C. R. Gould,[2] D. G. Haase,[2] J. N. Knudson,[1] G. E. Mitchell,[2] S. Penttilä,[1] H. Postma,[4] N. R. Roberson,[5] S. J. Seestrom,[1] J. J. Szymanski,[1,*] and X. Zhu[5]

(The TRIPLE Collaboration)

[1] *Los Alamos National Laboratory, Los Alamos, New Mexico 87545*

[2] *North Carolina State University, Raleigh, North Carolina 27695 and Triangle Universities Nuclear Laboratory, Durham, North Carolina 27706*

[3] *TRIUMF, Vancouver, British Columbia, Canada V6T 2A3*

[4] *University of Technology, Delft, The Netherlands*

[5] *Duke University, Durham, North Carolina 27706 and Triangle Universities Nuclear Laboratory, Durham, North Carolina 27706*

(Received 3 June 1991)

Parity nonconservation has been studied in the transmission of longitudinally polarized epithermal neutrons incident upon a ^{139}La target. Previous experiments have demonstrated the existence of a large value of the longitudinal asymmetry in the 0.734-eV p-wave resonance of the compound nucleus ^{140}La, but report conflicting values for the measured asymmetry. We report the results of an experiment at the Los Alamos Neutron Scattering Center (LANSCE) which measured the asymmetry by two independent methods. One of these methods utilizes a conventional polarizer and a single lanthanum target. The other method uses an unpolarized beam with two lanthanum targets, and therefore does not require a separate measurement of the beam polarization. The asymmetry values determined from these two methods (0.1015±0.0045 and 0.0955±0.0035, respectively) are compared to previously measured values. Measurement of the asymmetry of the 0.734-eV resonance in ^{139}La provides a highly accurate method of determining the polarization of an epithermal neutron beam.

I. INTRODUCTION

Parity nonconservation in a system of interacting nucleons has been studied in numerous experiments. One subset of these is the search for parity nonconservation in the resonance states of compound nuclei. Such efforts are attractive because of the existence of large enhancements, which can make parity-nonconserving effects readily observable [1–7]. Nuclei with nonzero spin which exhibit large parity-nonconserving (P-odd) effects are possible candidates for experimental tests for time-reversal (T) violation [8].

Recently [9] increased interest in parity violation in compound nuclei has resulted from experimental progress that allows measurement of parity nonconservation in a large number of p-wave resonances within the same nucleus. Statistical methods are then applicable to determine M, the root-mean-squared parity-violation matrix element. From M and the average level spacing D, one can calculate $\Gamma_{PV} = 2\pi M^2/D$, where Γ_{PV} is the parity-violation spreading width. Work by French [10] suggests that Γ_{PV} can be related to α_{PV}, the ratio of the P-odd to P-even effective NN interactions.

Since ^{139}La has only a few resonances at epithermal energies, at present it is not a suitable candidate for the determination of M. On the other hand, the large enhancement of parity violation in the 0.734-eV p-wave resonance of ^{139}La results in an effect [4–7] many orders of magnitude larger than the parity violation in the nucleon-nucleon interaction. This makes the 0.734-eV resonance of special interest as a candidate for T-violation experiments and as a standard analyzer for determining the polarization of epithermal neutron beams.

The helicity-dependent cross section for a given p-wave resonance can be written in the form

$$\sigma_{\pm} = \sigma(E)(1 \pm P) , \tag{1}$$

where $\sigma_{+\,(-)}$ is the cross section for + (−) helicity neutrons and $\sigma(E)$ is the helicity-independent p-wave neutron resonance cross section. The analyzing power P for a particular (the ith) p-wave resonance in the spectrum is given by [2, 9, 11, 12]

$$P_i = \sum_j \frac{2V_{ij}}{E_{sj} - E_{pi}} \frac{g^n_{sj}}{\sqrt{\Gamma^n_{pi}}} x_i , \tag{2}$$

where the summation is over all s-wave resonances that mix with the p-wave resonance being studied. V_{ij} is the weak-interaction matrix element for the mixing between the jth s-wave and the ith p-wave resonance states of the compound nucleus, $E_{sj} - E_{pi}$ is the energy separation of the two resonances, the partial neutron width amplitude for the jth s-wave resonance, g^n_{sj}, is a signed quantity with absolute magnitude $\sqrt{\Gamma^n_{sj}}$, and Γ^n_{sj} and Γ^n_{pi} are the neutron widths for the two resonances. The quantity x_i is the fractional contribution for the $j = \frac{1}{2}$ partial neutron width and is given by

$$x_i = g_{pi}^{n,1/2}/\sqrt{\Gamma_{pi}^n}\ ,$$

where

$$\Gamma_{pi}^{n,1/2} = (g_{pi}^{n,1/2})^2,\quad \Gamma_{pi}^n = \Gamma_{pi}^{n,1/2} + \Gamma_{pi}^{n,3/2}\ .$$

The ratio of matrix element to energy separation in Eq. (2) is usually referred to as the "dynamical" enhancement factor; for heavy nuclei with a high density of energy levels the enhancement over the single-particle value can be on the order of 300. The quantity $g_{sj}^n/\sqrt{\Gamma_{pi}^n}$ has a magnitude equal to the square root of the ratio of s-wave to p-wave neutron widths. At low energies, this "structural" enhancement factor is approximately the square root of the ratio of barrier penetrations of the l=0 and l=1 partial waves. This ratio is of order $1/kR$ and, in the 1-eV range, can provide an additional enhancement of 2–3 orders of magnitude. The x_i are quantities with range from -1 to 1, and on average are assumed not to effect qualitatively the magnitude of any total enhancement.

Results from previous experiments performed on ^{139}La at JINR [4], KIAE [5], and KEK [6] all have reported the observation of large effects which demonstrate the presence of a sizable enhancement. Although the measured values of the two Soviet experiments [4, 5] are consistent with each other, they disagree significantly (see Table I) with both KEK results, which were measured using two different techniques. A previous experiment [7] at Los Alamos was performed with the high-intensity pulsed neutron beam from the Los Alamos Neutron Scattering Center (LANSCE) but lacked sufficient precision to resolve the discrepancy. In the present paper we report new results for ^{139}La from experiments performed at LANSCE. The measurements consist of two separate experiments: one uses a conventional neutron polarizer to polarize the beam and the parity-violation asymmetry to analyze the beam (single lanthanum); the other uses the parity-violation asymmetry both to polarize and to analyze the beam (double lanthanum). The single-lanthanum experiment utilized a cryogenic neutron-spin filter in the same setup that is used by our collaboration in experiments [9] to measure M in other nuclei. The double-lanthanum experiment replaced the spin filter with a second lanthanum target, and polarized the beam via the weak interaction. This method results in a transmission asymmetry smaller than that in the single-lanthanum experiment by more than an order of magnitude. However, because the parity-violation asymmetry is used both to polarize and to analyze the beam, the double-lanthanum experiment is free of systematic uncertainties associated with the measurement of beam polarization.

TABLE I. Comparison of measurements of the parity asymmetry in the 0.734-eV resonance of lanthanum. The KEK(a) and KEK(b) values refer to neutron transmission and capture γ-ray measurements, respectively. Present works (a) and (b) refer to the single-lanthanum (a) and double-lanthanum (b) experiments described in this paper.

Group	P
JINR [4]	0.073 ± 0.005
KIAE [5]	0.076 ± 0.006
KEK(a) [6]	0.097 ± 0.005
KEK(b) [6]	0.095 ± 0.003
Los Alamos [7]	0.092 ± 0.017
Present work(a)	0.1015 ± 0.0045
Present work(b)	0.0955 ± 0.0035

II. SINGLE-LANTHANUM EXPERIMENT

A. Description

In the single-lanthanum experimental arrangement (Fig. 1), unpolarized neutrons produced at LANSCE were polarized using a cryogenically cooled polarized hydrogen target [13]. The n-p spin-spin cross section is large (16.7 b) and nearly constant from 1 eV to 50 keV, which makes polarized hydrogen a good neutron-beam polarizer. The neutrons of the beam are polarized in the same direction as the protons of the filter because the singlet n-p scattering cross section is much larger than the triplet cross section [14].

The neutron-spin filter consisted of single crystals of La_2(0.5% Nd)$Mg_3(NO_3)_{12}\cdot 24H_2O$ (LMN). The crystals formed a block 3.5 × 3.5 cm^2 in cross section by 1.78 cm thick, were cooled to 1.2 K in a pumped helium bath, and were situated in a longitudinal magnetic field of 2.02 T. The axis of the field was parallel to the beam. The protons in the crystals were polarized dynamically by irradiating them with microwaves. A microwave frequency of 75.520 GHz (75.684 GHz) was used to polarize the protons parallel (antiparallel) to the magnetic-field direction. During the course of the experiment, data were measured for both proton-spin directions in order to reduce the effects of possible systematic errors associated with the more frequent reversal of helicity produced by the spin flipper (described below). Proton polarizations of about 40% were achieved, which resulted in neutron polarizations of about 43%. In the region of the 0.734-eV resonance, a small amount of polarization estimated to be 0.06% is contributed by the weak interaction between the neutrons of the beam and the lanthanum of the LMN crystals. However, because the data were taken for both proton-spin directions, any effects on polarization due to the lanthanum in the spin filter tended to cancel over the

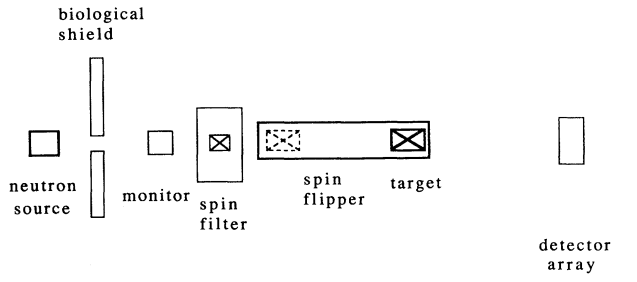

FIG. 1. Schematic of the experimental setup for the single-lanthanum experiment. For the double-lanthanum experiment, a second lanthanum sample (dotted line) was inserted at the front end of the spin flipper and the spin filter was removed.

course of the experiment.

A 1-mm-thick ^{6}Li glass scintillator paddle was placed between the LANSCE biological shield and the spin filter to provide a monitor of the total incident neutron flux in each 15-Hz beam burst. Beam polarization was monitored by measuring beam transmission through the polarizer, as well as by using nuclear magnetic resonance (NMR) techniques. The transmission of the spin filter was about 15%.

An adiabatic spin rotator [8] (referred to as the spin flipper) followed the polarizer and, depending on the magnetic-field settings of the spin flipper, allowed the spins of the beam neutrons to pass through either unchanged (*no flip*) or rotated by 180° (*flip*). The efficiency of the spin flipper was not quite 100% because a small transverse component of the solenoidal field caused a small fraction ϵ of the spins to be flipped while the spin flipper was in the *no-flip* state. The choice of a special eight-step spin sequence allowed the neutron helicity to be reversed in such a way that magnetic-field effects and time drifts were canceled through second order. We estimate that helicity-correlated changes in the spin-flipper magnetic fields affected the asymmetry measured in the neutron detector at a level smaller than 10^{-10}. The ^{139}La target (unpolarized) was located at the exit of the spin flipper, and consisted of room temperature La_2O_3 powder with lanthanum areal density of 0.065 atom/b. A small amount of water of crystallization in the powder attenuated the neutron flux by about a factor of 10, but otherwise did not affect the determination of the lanthanum resonance asymmetry.

The experiment measured parity violation as a helicity-correlated difference in the number of transmitted neutrons. The detector array consisted of seven 1.0 cm thick, 13.0 cm in diameter cylindrical ^{6}Li glass scintillators optically coupled to photomultiplier tubes. Six of the seven detector units were positioned in a circle of 0.4 m in diameter with the seventh in the center of the circle. Individual high-voltage supplies were used for each of the final four dynode stages to supply high currents to these dynodes. This prevented high counting rates from changing the photomultiplier gains. The array was located at a flight-path distance of 56 m from the LANSCE source. Detected neutrons were counted in pulse mode by a Canberra model 7880 100-MHz multiscaler operating with a dwell time of 1 μsec. The Canberra multiscaler was interfaced to a CAMAC-based DSP model 6001 signal-averaging memory. The neutron spins were flipped every 10 sec by the spin flipper; each data run, lasting about one half hour, consisted of 20 eight-step sequences. Any eight-step sequence (200 beam pulses) for which the monitor detector showed beam intensity fluctuations of greater than 8% was rejected. This amounted to about one-fourth of the data. The CAMAC system used for data acquisition was controlled by a MicroVAX II computer.

For neutrons transmitted by the polarizer (see Fig. 2) the neutron polarization is given by the quantity f_n, where

$$f_n = \frac{N_1^+ - N_1^-}{N_1^+ + N_1^-} .$$

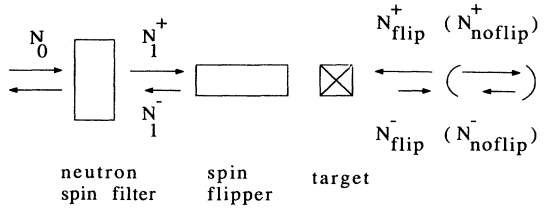

FIG. 2. Transmission of neutron spins through the neutron spin filter, spin flipper, and lanthanum target. N_0 is the number of incident neutrons. N_1^+ (N_1^-) is the number of + (−) helicity neutrons transmitted by the polarizer, N^+_{flip} (N^-_{flip}) is the number of positive (negative) helicity neutrons transmitted through the target when the spin flipper is on, and $N^+_{no\ flip}$ ($N^-_{no\ flip}$) is the number of positive (negative) helicity neutrons transmitted through the target when the spin flipper is off.

Here N_1^+ (N_1^-) is the number of + (−) helicity neutrons transmitted by the polarizer. The polarizer was followed by the spin flipper and an unpolarized target which, in the case of parity nonconservation, is characterized by helicity-dependent scattering cross sections σ_+ and σ_-. For the case of a 100% efficient spin flipper, with the helicity-dependent scattering cross sections σ_+ and σ_-. For the case of a 100% efficient spin flipper, with the spin flipper off (*no flip*) the number of positive (negative) helicity neutrons transmitted through a target of areal density n is $N^+_{no\ flip}$ ($N^-_{no\ flip}$), where

$$N^+_{no\ flip} = N_1^+ e^{-\sigma_+ n}$$

and

$$N^-_{no\ flip} = N_1^- e^{-\sigma_- n} .$$

This leads to a total number of neutrons transmitted of

$$N^{tot}_{no\ flip} = (N_0/2)\left[(1+f_n)e^{-\sigma_+ n} + (1-f_n)e^{-\sigma_- n}\right] ,$$

where $N_0 = N_1^+ + N_1^-$. Similarly, for the *flip* case

$$N^{tot}_{flip} = (N_0/2)\left[(1-f_n)e^{-\sigma_+ n} + (1+f_n)e^{-\sigma_- n}\right] .$$

One can enter the helicity dependence of the cross section explicitly by using Eq. (1). In an experiment which studies the helicity-dependent transmission in the region of a compound-nuclear resonance, the yields Y_{flip} and $Y_{no\ flip}$ for the *flip* and *no-flip* cases become

$$Y_{flip} = N_0 C(E) e^{-\sigma(E)n}[\cosh(x) + f_n \sinh(x)] \quad (3)$$

and

$$Y_{no\ flip} = N_0 C(E) e^{-\sigma(E)n} \times[\cosh(x) - (1-2\epsilon) f_n \sinh(x)] , \quad (4)$$

where $x = \sigma(E) n P$. A correction for spin-flipper inefficiency ϵ has been incorporated into the expression for $Y_{no\ flip}$ that appears in Eq. (4). The factor $\sigma(E)$ represents the resonance line shape, ϵ is the fraction of spins that are flipped when the spin flipper is in the *no-flip* state, and $C(E)$ is the energy-dependent line shape of the nonresonant neutron flux (including contributions from the detector efficiency). The neutron moderator pro-

duces a flux which varies approximately as $1/E$. Hence $C(E)$ can be written as

$$C(E) = dN/dE$$
$$= (\alpha/E)\left(1 + \sum_i b_i(1/\sqrt{E} - 1/\sqrt{E_0})^i\right) . \quad (5)$$

Since the detector efficiency has a $1/v$ dependence, the deviation of $C(E)$ from $1/E$ behavior is expressed as a power series in $1/\sqrt{E}$. E_0 is an arbitrarily chosen energy.

In the limit that $x \ll 1$, Eqs. (3) and (4) can be written as

$$Y_{flip} = N_0 C(E) e^{-\sigma(E) n (1 - f_n P)}$$

and

$$Y_{no\ flip} = N_0 C(E) e^{-\sigma(E) n [1 + (1-2\epsilon) f_n P]} .$$

Only if the neutron polarization f_n is accurately measured can the *flip* and *no-flip* resonance line shapes be analyzed to yield an accurate value of the parity-violation asymmetry P.

B. Measurement of polarization

The neutron polarization f_n is derived from the LMN proton polarization f_p via

$$f_n = \tanh[f_p(\sigma_P - \sigma_A) n/2] , \quad (6)$$

where n is the areal density of the polarized hydrogen in the LMN crystal (1.16 atom/b), and σ_P (σ_A) is the n-p cross section for parallel (antiparallel) neutron-proton spins. The proton polarization was monitored via an NMR coil wrapped around the surface of the LMN-crystal block. In principle f_p is obtained absolutely by comparing the enhanced NMR-absorption signal area with a signal area measured at thermal equilibrium [13]. We found that f_p was underestimated by this method, possibly due to surface damage to the crystals. Therefore we calibrated the NMR signal by fitting transmission yield versus NMR area for data taken with the LMN target polarized and unpolarized. The calibration method used was based on one outlined in Ref. [15], and relies on the fact that the polarized to unpolarized transmission ratio through the LMN is given by $\cosh[f_p(\sigma_P - \sigma_A) n/2]$.

Our calibration method measured transmission through the spin filter in a series of runs that began as soon as the microwave power was turned off. The proton spin-lattice relaxation time for LMN crystals at 1.2 K and 2.02 T is about 15 min. As f_p relaxes to zero, the transmission falls by about 20%. The transmission was determined by calculating the ratio of the signal from the lithium-glass array located at 56 m to that of the monitor detector. For these transmission measurements, the spin flipper was turned off and the lanthanum target was removed. Transmission yields were measured at 2-min intervals. In Fig. 3 the averages of NMR signals taken before and after each run are compared to the corresponding transmission yields. A fit of the form

$$T = a_1 \cosh(a_2 S_{\rm NMR}) + a_3 s + a_4 s^2 ,$$

where T is the transmission, $S_{\rm NMR}$ is the area of the NMR signal, and s is the time, was made to the transmission data and is also presented in Fig. 3. The fit variable a_1 represents the polarization-independent attenuation of the spin filter, a_2 is the ratio of $[f_p(\sigma_P - \sigma_A)n]/2$ to $S_{\rm NMR}$, and a_3 and a_4 are constants characterizing first- and second-order time drifts. From the fit, a_2 was determined to 3% accuracy. In a separate run, a thin tantalum sample was inserted in the beam to obtain a background determination at a neutron energy of 4.28 eV, where there is a black resonance in the tantalum spectrum.

When transmission is used to determine the proton polarization of the spin filter, the wrong polarization value can be inferred if the polarization is not uniform across the transmitted beam. If the beam direction lies in the plane of the crystals, then a spatially dependent polarization can be produced if either ineffective crystals or gaps between the crystals are present, or the polarization decays with different rates in different crystals. The spin-filter cross sections for antiparallel spins and for parallel spins can be represented by (σ_A) and (σ_P), respectively. The transmission T for a spin filter of areal density n and of uniform polarization f_P is then given by
given by

$$T = T_0 \cosh[f_p(\sigma_P - \sigma_A) n/2] ,$$

where T_0 represents the polarization-independent attenuation of the neutron beam in the spin filter. The resulting neutron polarization f_n is given by Eq. (6). If the spin filter has uniform polarization and $y = f_p(\sigma_P - \sigma_A)t/2 \ll 1$, then the normalized transmission $T' = T/T_0$ is given by

$$T' = \cosh(y) \cong 1 + y^2/2 \quad (7)$$

and

$$f_n = \tanh(y) \cong y = [2(T' - 1)]^{1/2} .$$

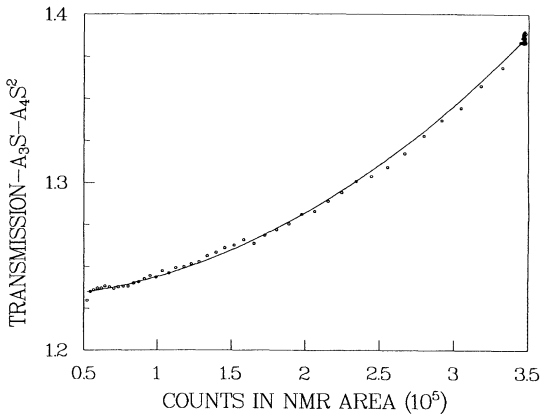

FIG. 3. The change in time-corrected transmission yields vs NMR area as the neutron-spin filter used in the single-lanthanum experiment was depolarized. A fit (solid line) of the functional form $T = a_1 \cosh(a_2 S_{\rm NMR}) + a_3 s + a_4 s^2$ was made to the data (see text) in order to determine the spin-filter polarization.

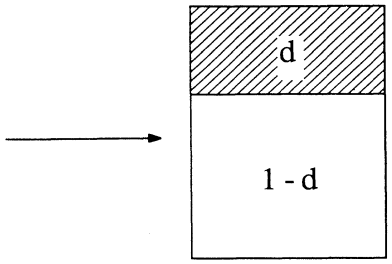

FIG. 4. Example of a polarizer which produces nonuniform polarization. The polarizing sample has a fraction d of crystals which are unpolarized, and a remainder $1-d$ which are polarized.

Since y enters quadratically in T', the transmission measures the mean-squared polarization of the beam. If the polarization is nonuniform, the mean-squared polarization will always be larger than the square of the mean polarization. Thus the transmission method can imply a polarization value that is larger than the actual mean polarization of the beam.

As a specific example consider the situation shown in Fig. 4, where the polarizing sample has a fraction d of crystals which produce no polarization. The true neutron polarization, f_n^{true}, produced by such a sample is

$$f_n^{\text{true}} = (1-d)y \ ,$$

and the measured T' is

$$T'_{\text{true}} = (1-d)(1+y^2/2) + d = 1 + \frac{(1-d)}{2}y^2 \ .$$

However, if one mistakenly believes the crystals to be uniformly good, then the measured T' will result in an incorrectly deduced polarization:

$$f_n^{\text{deduced}} = [2(T'_{\text{true}} - 1)]^{1/2} = [(1-d)y^2]^{1/2} = \sqrt{1-d}\,y,$$

which will differ from the true polarization by a factor of

$$\frac{f_n^{\text{true}}}{f_n^{\text{deduced}}} = \frac{(1-d)y}{(\sqrt{1-d})y} = \sqrt{1-d}$$

and would lead to an incorrect value for the calculated parity asymmetry P. Since agreement was obtained (see below) between the single-lanthanum and double-lanthanum (polarization-independent) results, we conclude that there was no significant spatially nonuniform polarization in the single-lanthanum measurement.

C. Single-lanthanum results

A total of 47 runs was accumulated, and Fig. 5 shows the 0.734-eV resonance peak for the sum of the two different neutron helicities. The asymmetry in the sum data is also shown in the figure. Each run was analyzed separately by fitting to histograms of yield versus time of flight, t. For both *flip* and *no flip*, these histograms

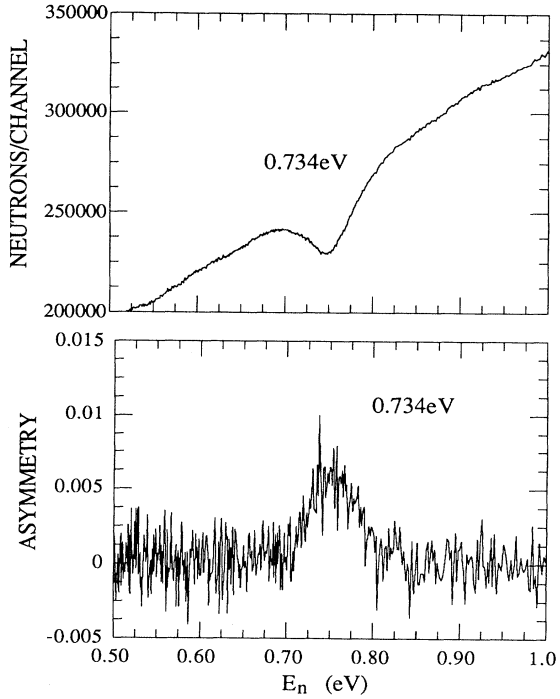

FIG. 5. The top graph shows, for the single-lanthanum runs, the transmitted neutron yield as a function of energy in the vicinity of the ^{139}La 0.734-eV resonance. Below, for the same energy range, is plotted the asymmetry $(Y_{flip} - Y_{no\ flip})/(Y_{flip} + Y_{no\ flip})$ for data taken with a beam of net positive helicity exiting the spin polarizer. Flip (*no flip*) refers to a state whereby the spins passing through the spin flipper are reversed (not reversed).

(referred to henceforth as spectra) were fit to Doppler-broadened Breit-Wigner resonances of different amplitude which multiplied identical polynomial expressions for the nonresonant flux:

$$Y_{flip} = N_{flip}C(E)e^{-\sigma(E)n(1-f_nP)} \tag{8}$$

and

$$Y_{no\ flip} = N_{no\ flip}C(E)e^{-\sigma(E)n[1+(1-2\epsilon)f_nP]} \ , \tag{9}$$

where $C(E)$ is given by Eq. (5), N_{flip} and $N_{no\ flip}$ are the overall normalizations, and $\sigma(E)$ is the Doppler-broadened energy-dependent cross section given by

$$\sigma(E) = \frac{\sigma_0}{\sqrt{\pi}}\int_0^\infty \sqrt{\frac{E}{E_0}}\frac{\exp[-(E-E')^2/\Delta^2]}{\Delta\left[1+\left(\frac{(E'-E_0)}{\Gamma/2}\right)^2\right]}dE' \ . \tag{10}$$

Here E is the neutron energy relative to a stationary nucleus, E' is the neutron energy relative to the moving nucleus, E_0 is the neutron energy at the peak of the resonance, $\Delta = \sqrt{4E_0kT_e/A}$, A is the atomic weight of the target nucleus, k is the Boltzmann constant, T_e is an effective temperature characterizing the target, and σ_0 and Γ are parameters characteristic of the nonbroadened

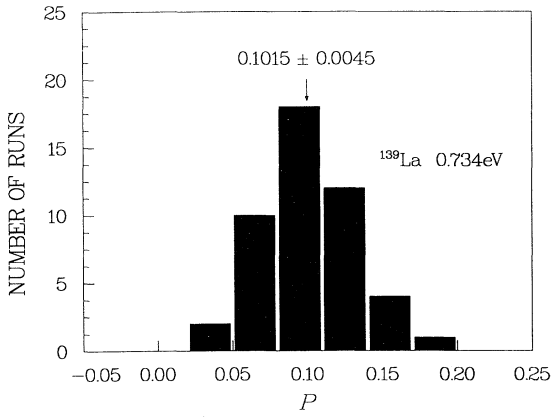

FIG. 6. Histogram of the measured parity-violation asymmetry values from individual single-lanthanum runs.

resonance shape.

The b_i factors contained in the expression for $C(E)$ [see Eq. (5)] parametrize the change in flux and detector efficiency across the resonance. The parity-violation effect is given by the product of P and the neutron polarization f_n. The parameters σ_0, b_i, E_0, Γ, and T_e are determined from the data by a fit to the parity-nondependent sum $Y_{flip} + Y_{no\ flip}$. The measured parity asymmetry $P = (\sigma_+ - \sigma-)/(\sigma_+ + \sigma_-)$ does not itself explicitly depend on σ_0, nor on any of the other resonance shape parameters. The value of P enters into the equations for Y_{flip} and $Y_{no\ flip}$ as a multiplicative factor to a function of line-shape parameters. Therefore, while a determination of P does depend on a precise determination of the parity-nondependent line shape, it does not depend on a precise determination of any single line-shape parameter, and any combination of shape parameters which result in an accurate fit to $Y_{flip} + Y_{no\ flip}$ will allow an accurate determination of the parity-violating asymmetry.

The actual fits were made with ϵ set equal to zero, and the extracted values of P were later divided by the factor $(1 - \epsilon)$ to correct for spin-flipper inefficiency. The parity asymmetries of individual runs yield the values of P plotted in Fig. 6. The spin-flipper inefficiency ϵ was calculated to be 0.006. The individual values of Fig. 6 result in an average parity-violation analyzing power P of

$$P = 0.1015 \pm 0.0045 ,$$

where the error is obtained by adding in quadrature the variance of the individual $f_n P$ values to the 3% uncertainty in the neutron polarizations.

III. DOUBLE LANTHANUM

A. Description

In the double-lanthanum experiment, the cryogenic polarizer was removed and replaced by a second ^{139}La target. This arrangement utilizes the parity-violation asymmetry occurring in the first target to produce a weakly polarized beam for helicity-dependent measurement on the second target. Because the weak interaction is used to polarize the beam, this method of performing the experiment can only be performed in the presence of very high neutron fluxes and with a target such as ^{139}La, where the nuclear enhancements are large. The advantage of this method is that the helicity-dependent cross section can be extracted directly from the measured transmission asymmetry without introducing systematic errors from an incorrect measurement of the beam polarization.

The polarizer and target samples for the double-lanthanum experiment were matched disks of ^{139}La metal, each 5.105 cm thick and 5.080 cm in diameter. Each disk was held in a vacuum vessel to prevent oxidation, and the upstream sample was surrounded by a brass collimator to prevent neutrons that had not passed through the lanthanum from reaching the detectors. The samples were located one at each end of the spin-flip solenoid in such a way that each sample was inside the solenoidal guide field. This ensured that any polarization produced in the upstream sample was maintained into the spin-flip region and that the spin exiting the spin-flip region was maintained up to the second sample. The LANSCE source of pulsed neutrons was effectively a distance of 6.7 m from the upstream La sample. At the biological shield, a distance of 4.6 m in front of the upstream sample, the beam was collimated to a diameter of 5.08 cm. The two lanthanum samples were separated by a distance of 2 m.

The same detector array described above in the single-lanthanum section was used for these measurements. Because of the higher counting rates, data were acquired in an integral counting mode [16] using a DSP 6012, 12 bit, transient digitizer in conjunction with a DSP 4101 signal-averaging memory. The transient digitizer was operated at a dwell time of 1 μs per channel, and the detector output signals were conditioned by a low-pass filter with a time constant that matched the dwell time of the digitizer.

In the double-lanthanum setup, the number of positive (negative) helicity neutrons N_1^+ (N_1^-) exiting the first lanthanum sample is given by

$$N_1^{\pm} = (N_0/2)e^{-\sigma_{\pm} n_1} ,$$

where n_1 is the areal density of the first lanthanum sample. The yields Y_{flip} and $Y_{no\ flip}$ for *flip* and *no flip* are derived by substituting

$$(1 + f_n) = e^{-\sigma_+ n_1}, \quad (1 - f_n) = e^{-\sigma_- n_1},$$

into Eqs. (3) and (4). In the case where the two lanthanum samples are of equal areal densities, n, the yields become

$$Y_{no\ flip} = N_0 C(E) e^{-2\sigma_0 n} \cosh[2\sigma_0 n P(1 - \epsilon/2)]$$

and

$$Y_{flip} = N_0 C(E) e^{-2\sigma_0 n} .$$

B. Double-lanthanum results

A total of 79 data runs were analyzed from the seven-detector/transient-digitizer combination at 56 m. In addition, five runs were taken in pulse-counting mode to aid in accurately determining the resonance line shape. In the pulse-counting runs, individual detector pulses underwent pulse-height discrimination and were counted using the same Canberra model 7880 multiscaler that was used in the single-lanthanum experiment. The pulse-counting detector was a 1-cm diameter ^{6}Li detector placed at a distance of 22.3 m from the LANSCE neutron source. It was placed at the shorter flight-path distance to increase the counting rate.

The sum of the multiscaler *flip* spectra was fit to a parity-independent resonance line shape of the form

$$Y_{flip}^{\mathrm{MS}} = N_0 C(E) e^{-2\sigma(E)n} ,$$

where n is the areal density of each target, $C(E)$ is the nonresonant flux given by Eq. (5), and $\sigma(E)$ is the Doppler-broadened energy-dependent cross section given by Eq. (10).

In the next step, the sum of all transient-digitizer *flip* runs was fit to the form

$$Y_{flip}^{\mathrm{TD}} = N_0 C(E)[e^{-2\sigma(E)n} + B] ,$$

where $C(E)$ and $\sigma(E)$ were fixed to be the line shapes determined in the fits to the double-lanthanum multiscaler data. This fit quantitatively determined B, the nonresonant background term in the spectrum of the transient digitizer whose input pulses are not discriminated on the basis of pulse height. The subsequent analysis is rather insensitive to the value of B.

Finally, the ratio of the *no-flip* to *flip* spectra for the double-lanthanum transient digitizer runs is

$$\frac{Y_{no\ flip}}{Y_{flip}} = \alpha \frac{e^{-2\sigma n}\cosh[2\sigma n P(1-\epsilon/2)] + B}{e^{-2\sigma n} + B} . \qquad (11)$$

Because of a different beam size, the spin-flipper inefficiency ϵ was larger for the double-lanthanum runs than for the single-lanthanum runs. For the double-lanthanum runs ϵ has been calculated to be 0.020. For each run, the ratio of the $Y_{no\ flip}$ spectrum to the Y_{flip} spectrum was computed and fit with the functional form of Eq. (11) to extract the parity-violation asymmetry P. The actual fit was performed using the approximation $\cosh[2\sigma n P(1-\epsilon/2)] \cong 1 + 2[\sigma n P(1-\epsilon/2)]^2$, and P^2 was used as the fit variable. If a direct fit is made to $\cosh[2\sigma n P(1-\epsilon/2)]$, then an incorrect result is obtained because the cosh function is constrained to be positive. Figure 7 shows the fit of the functional form given by Eq. (11) to the sum of all 79 runs. The result for P^2 from the double-lanthanum experiment is

$$P^2 = 0.008\,94 \pm 0.000\,95 .$$

A set of 43 target-empty runs was performed and analyzed as a control. Any false asymmetry in the double-lanthanum experiment also should appear in the target-empty runs. The target-empty runs give

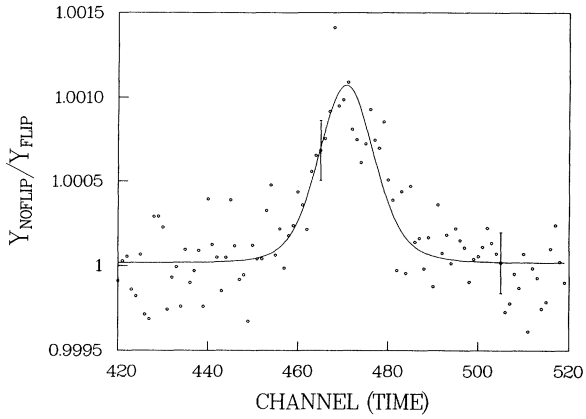

FIG. 7. Parity-violation asymmetry in the 0.734-eV resonance of ^{139}La for the sum of all 79 double-lanthanum data runs. The ratio $Y_{no\ flip}/Y_{flip}$ is plotted as a function of energy, and the parity violation is seen in the deviation of the ratio from 1.0 near the center of the resonance. Representative errors for the uncertainties in each data point are drawn in on data points in the peak region and outside the peak region.

$$P^2 = -0.000\,03 \pm 0.000\,79 ,$$

which shows that if any false asymmetry is present, it is smaller than the statistical error of the target-in runs.

From the measured value of P^2 with target in, the parity-violation asymmetry $|P|$ is

$$|P| = 0.0955 \pm 0.0035.$$

IV. DISCUSSION

The results of the single-lanthanum experiment agree with those of the double-lanthanum experiment. Both results are also in agreement with the previously measured KEK values.

The lanthanum measurements fall within the framework of an experimental program whose goal is to measure parity nonconservation in the epithermal p-wave resonances of a wide range of heavy nuclei. Such a survey will determine whether the nuclear medium alters the effect of the basic nucleon-nucleon interaction, and at the same time, will search for suitable candidate targets for use in a planned time-reversal experiment [8]. The survey utilizes a cryogenic polarizer to achieve a high flux of polarized neutrons, and this requires an accurate knowledge of the polarization produced by the polarizer in order to determine correctly the parity asymmetries. A technique such as NMR can be used to monitor changes in the polarization on a continuous basis, but an accurate calibration is still required to determine the absolute polarization. Using the method of measuring transmission through the polarizer to determine polarization can

give incorrect values if the polarization is nonuniform across the beam. To determine the beam polarization one can measure the parity-violation asymmetry by the single-lanthanum method and compare this value to the asymmetry which has been measured by the polarization-independent double-lanthanum method. This comparison approach is probably the most accurate method of determining this calibration.

ACKNOWLEDGMENTS

This work was supported in part by the U.S. Department of Energy, Office of High Energy and Nuclear Physics, under Contracts No. DE-AC05-76ER01067 and No. DE-FG05-88ER40441, and by the U.S. Department of Energy, Office of Energy Research, under Contract No. W-7405-ENG-36.

* Present address: Indiana University, Bloomington, Indiana 47405.

[1] Yu. G. Abov, P. A. Krupchitsky, and Yu. A. Oratovsky, Phys. Lett. **12**, 25 (1964); Yad. Fiz. **1**, 479 (1965) [Sov. J. Nucl. Phys. **1**, 341 (1965)].

[2] O. P. Sushkov and V. V. Flambaum, Usp. Fiz. Nauk **136**, 3 (1982) [Sov. Phys. Usp. **25**(1), 1 (1982)].

[3] V. E. Bunakov and V. P. Gudkov, Nucl. Phys. **A401**, 93 (1983).

[4] V. P. Alfimenkov, S. B. Borzakov, Vo Van Thuan, Yu. D. Mareev, L. B. Pikelner, A. S. Khrykin, and E. I. Sharapov, Nucl. Phys. **A398**, 93 (1983).

[5] S. A. Biryukov, L. N. Bondarenko, S. V. Zhukov, Yu. V. Zakharov, V. M. Zykov, V. L. Kuznetsov, P. V. Malankin, V. I. Mostovoi, A. A. Osochnikov, S. P. Pugachev, V. I. Raitsis, and A. N. Chernyi, Yad. Fiz. **45**, 1511 (1987) [Sov. J. Nucl. Phys. **45**, 937 (1987)].

[6] Y. Masuda, T. Adachi, A. Masaike, and K. Morimoto, Nucl. Phys. **A504**, 269 (1989).

[7] C. D. Bowman, J. D. Bowman, and V. W. Yuan, Phys. Rev. C **39**, 1721 (1989).

[8] J. D. Bowman, C. D. Bowman, J. Knudson, S. Penttilä, S. J. Seestrom, J. J. Szymanski, V. W. Yuan, C. R. Gould, D. G. Haase, G. E. Mitchell, N. R. Roberson, P. P. J. Delheij, H. Postma, and E. D. Davis, in *Fundamental Symmetries in Nuclei and Particles*, edited by H. Henrikson and P. Vogel (World Scientific, Singapore, 1989), p.1.

[9] J. D. Bowman, C. D. Bowman, J. E. Bush, P. P. J. Delheij, C. M. Frankle, C. R. Gould, D. G. Haase, J. Knudson, G. E. Mitchell, S. Penttilä, H. Postma, N. R. Roberson, S. J. Seestrom, J. J. Szymanski, V. W. Yuan, and X. Zhu, Phys. Rev. Lett. **65**, 1192 (1990).

[10] J. B. French, V. K. B. Kota, A. Pandey, and S. Tomsovic, Ann. Phys. (N.Y.) **181**, 198 (1988).

[11] J. R. Vanhoy, E. G. Bilpuch, J. F. Shriner, Jr., and G. E. Mitchell, Z. Phys. A **331**, 1 (1988).

[12] C. R. Gould, D. G. Haase, N. R. Roberson, H. Postma, and J. D. Bowman, Int. J. Mod. Phys. A **5**, 2181 (1990).

[13] G. A. Keyworth, J. R. Lemley, C. E. Olsen, and F. T. Seibel, Phys. Rev. C **8**, 2352 (1973).

[14] V. I. Lushchikov, Yu. V. Taran, and F. L. Shapiro, Yad. Fiz. **10**, 1178 (1969) [Sov. J. Nucl. Phys. **10**, 669 (1970)].

[15] D. Draghicescu, V. I. Lushchikov, V. G. Nikolenko, Yu. V. Taran, and F. L. Shapiro, Phys. Lett. **12**, 334 (1964).

[16] J. D. Bowman, J. J. Szymanski, V. W. Yuan, C. D. Bowman, A. Silverman, and X. Zhu, Nucl. Instrum. Methods **A297**, 183 (1990).